



Short communication

Electrochemical instability of LiV_3O_8 as an electrode material for aqueous rechargeable lithium batteries

A. Caballero, J. Morales*, O.A. Vargas

Departamento de Química Inorgánica e Ingeniería Química, Universidad de Córdoba, Edificio Marie Curie, Campus de Rabanales, 14071 Córdoba, Spain

ARTICLE INFO

Article history:

Received 11 November 2009

Accepted 17 January 2010

Available online 25 January 2010

Keywords:

Vanadium oxide

Lithium cells

Aqueous batteries

ABSTRACT

We demonstrate the unsuitability of LiV_3O_8 as an electrode material for aqueous rechargeable lithium batteries on simple but solid grounds: the compound is unstable under typical battery operation conditions, where it slowly dissolves as reflected in the yellow color acquired by the electrolyte. This can be the origin of the poor performance of the aqueous batteries based on this compound.

© 2010 Elsevier B.V. All rights reserved.

1. Introduction

The outstanding papers by Dahn et al. [1,2] on aqueous rechargeable lithium batteries (ARLB) encouraged research into ways of improving their poor performance by increasing their delivered capacity and life cycle [3–7]. Using an appropriate electrode material is obviously an essential pre-requisite to succeed in this respect. Several years ago, the layered phase LiV_3O_8 was proposed by Köhler et al. [8] as anode material for these electrochemical devices. Recently, Wu and coworkers have emphasized the suitability of this compound against a wide variety of cathodic materials such as LiCoO_2 [9,10], LiMn_2O_4 [11] and $\text{LiNi}_{1/3}\text{Co}_{1/3}\text{Mn}_{1/3}\text{O}_2$ [12]. The results, however, were somewhat disappointing since the capacity faded continuously upon cycling.

In order to shed some light on the origin of this shortcoming, we performed a systematic study of the influence of different variables starting from particle size. However, we found the origin of the poor battery performance to be related neither with this nor with any other structural property, but rather with the instability of this layered oxide in contact with water. In fact, LiV_3O_8 tends to dissolve under the battery operating conditions. Our results are consistent with the observations made by Li and Dahn [13], who ascribed capacity fading in an aqueous lithium ion battery to dissolution of the active material.

2. Experimental

LiV_3O_8 was obtained in two particle sizes: micrometric (m-LiVO) and submicrometric (sm-LiVO). The micrometric sample was prepared from a mixture of Li_2CO_3 and V_2O_5 (both from Merck). 10% excess of Li precursor was used and the product calcined at 600°C for 48 h. On the other hand, sm-LiVO, was synthesized from precursors $\text{Li}(\text{CH}_3\text{-COO})$ (also in a 10% in excess) and $\text{VO}(\text{C}_5\text{H}_8\text{O}_2)_2$ (both from Aldrich). Oxalic acid from Aldrich was added to the precursor mixture in a 2:1 mole ratio in order to reduce particle size [14]. The final mixture was heated at 120°C for 5 h and then at 500°C for a further 5 h. LiMn_2O_4 was also obtained in two different particle sizes. The method used to prepare highly crystalline nanometric particles around 40 nm in size (n-LMO) is described elsewhere [15]. The spinel with micrometric particle size (1–2 μm) was obtained by applying a conventional ceramic procedure to a stoichiometric mixture of Li_2CO_3 (Fluka) and $\text{Mn}(\text{C}_5\text{H}_7\text{O}_2)_3$ (Strem Chemicals) that was then calcined in the air at 900°C for 24 h. Both samples were obtained as highly pure spinels, as revealed by their XRD patterns (not shown).

XRD patterns were recorded on a Siemens D5000 X-ray diffractometer using non-monochromated $\text{Cu K}\alpha$ radiation and a graphite monochromator for the diffracted beam. The scanning conditions were $5\text{--}90^\circ$ (2θ), a 0.03° step size and 12 s per step. Transmission electron microscopy (TEM) images were obtained with a Phillips TEM instrument operating at 100 keV and SEM images with a Jeol 6400 scanning electron microscope.

Electrochemical measurements were carried out in a three-electrode cell with Pt wire as counterelectrode and saturated calomelane (SCE) (supplied by CHI Instruments) as reference electrode. The working electrode was prepared by mixing 80 wt%

* Corresponding author. Tel.: +34 957 218620; fax: +34 957 218621.
E-mail address: iq1mopaj@uco.es (J. Morales).

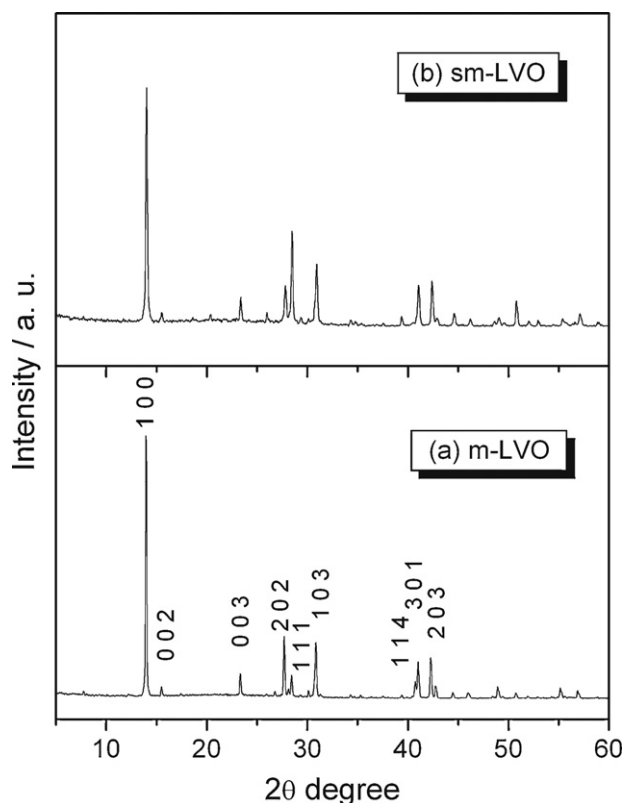


Fig. 1. XRD patterns for the LiV_3O_8 samples. (a) m-LVO; (b) sm-LVO.

of active material with 10wt% Super P carbon black (Timcal) and 10wt% PVDF (Aldrich). The mixture was pressed into either stainless steel grid or Ni mesh at 250 MPa for 20 min. A 1 M LiNO_3 aqueous solution was used as electrolyte. Cyclic voltammetry was conducted at a scan rate of 0.1 mV s^{-1} . The potential range was -0.3 to 1.1 V , which is outside the region for water decomposition. Measurements were made with a Solartron potentiostat–galvanostat model 1286. Galvanostatic cycling tests were carried out in a two-electrode Swagelok-type cell under different charge/discharge regimes (from C/5 to 5C, C representing 1 Li^+ ion exchanged in 1 h, equivalent to 148 mAh g^{-1} in the case of the Li–Mn spinel and 2 Li^+ , equivalent to 272 mAh g^{-1} for the V-based compound). Measurements were made over the voltage window 0.0 – 1.5 V on an Arbin BT2000 potentiostat–galvanostat system.

3. Results and discussion

Fig. 1 shows the XRD patterns for the two samples of LiV_3O_8 . The positions of the diffraction peaks matched those for the layered-type LiV_3O_8 quite well and the lattice constants ($a = 6.693 \text{ \AA}$, $b = 3.595 \text{ \AA}$, $c = 11.333 \text{ \AA}$) were consistent with those reported values (JCPDS card 72-1193). Therefore, both synthetic procedures yielded LiV_3O_8 of a high purity and crystallinity. It is worth noting the increased intensity of the (100) reflection relative to the other peaks and, particularly, the (111) reflection. The difference was especially significant for the micrometric sample. This reflects a tendency to grow preferentially along [100], as confirmed by the electron microscopy images.

Particle shape was consistent with anisotropic growth as deduced from XRD data. The particles of the m-LVO sample, Fig. 2a, were clearly needle-shaped, 10 – $25 \mu\text{m}$ in length and 2 – $3 \mu\text{m}$ in width. sm-LVO particles were also needle-shaped but its rods were shorter and thinner. Based on its TEM images, Fig. 2b, particles were

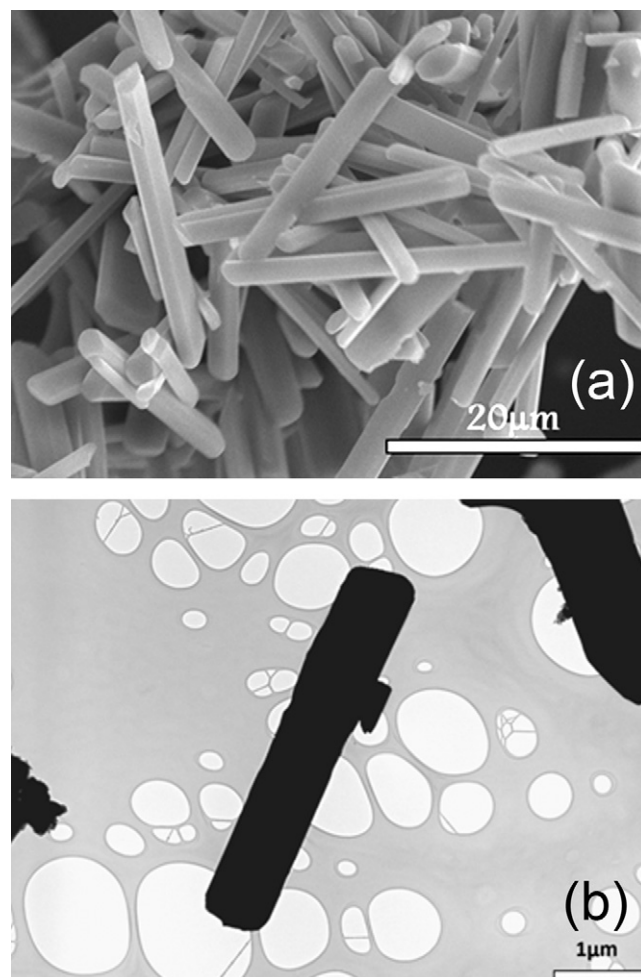


Fig. 2. (a) SEM image of sample m-LVO. (b) TEM image of sample sm-LVO.

less than $10 \mu\text{m}$ long and around $0.5 \mu\text{m}$ wide. The label was based on the latter dimension.

The CV curve for m-LVO sample was as expected [8,9], Fig. 3a, and exhibited a two redox peaks assigned to the Li^+ ion insertion/extraction reaction. The higher intensity of the peak belonging to the latter reaction, commonly found in V-based oxides [12,16], might be indicative of the instability of this compound under the conditions of the electrochemical measurements. Conclusive evidence in support of this argument was provided by the color change in the solution: from colorless (before the curve was recorded) to yellow (after the cyclic voltammogram was obtained), the color being typical of VO_2^+ in aqueous solutions (see Fig. 4). This is consistent with the tendency of LVO compounds to dissolve under a current flow. In fact, no color change was observed at open circuit. The sm-LVO sample exhibited a similar behavior, so particle size cannot be the origin of instability. The mechanism behind such instability is unknown at present, but it might involve the co-intercalation of water molecules at the time of lithium insertion into the structural framework. The structural expansion required may introduce strong stress and cause the structure to collapse, thereby facilitating dissolution.

This electrode degradation phenomenon and its adverse effect on cell performance in a real-life battery were checked by using the LiMn_2O_4 spinel as positive electrode. The electrochemical response of this spinel in a half-cell (Pt wire as counterelectrode), irrespective of this particle size, yielded the two well-known peaks associated to the $\text{Mn}^{3+}/\text{Mn}^{4+}$ pair redox and the extraction and insertion of Li, respectively (Fig. 3b) [17]. However, the reduction

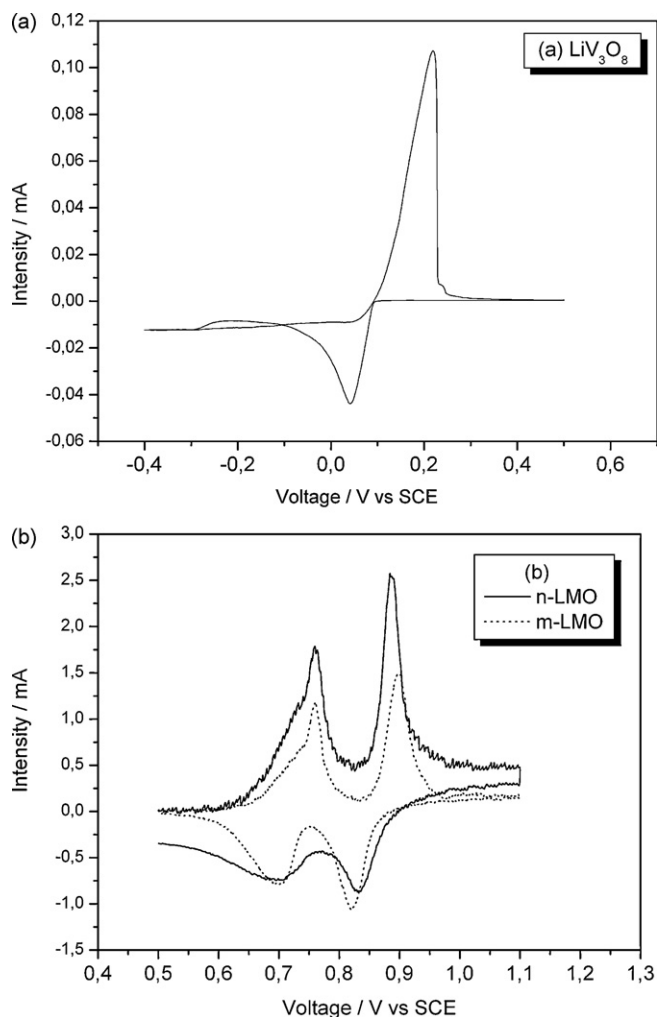


Fig. 3. Cyclic voltammograms. (a) LiV_3O_8 ; (b) LiMn_2O_4 .

peaks for the n-LMO sample were broader and more ill-defined, which suggests a lower reversibility in the lithium extraction and insertion reaction. This result is somewhat surprising since the smaller particle size should have facilitated Li-ion transport along the shortened diffusion paths [18]. However, nanometric particles increased the electrode/electrolyte contact area and may facilitate side reactions. In this situation, dissolution of the spinel cannot be ruled out, but confirming this assumption would require analyt-

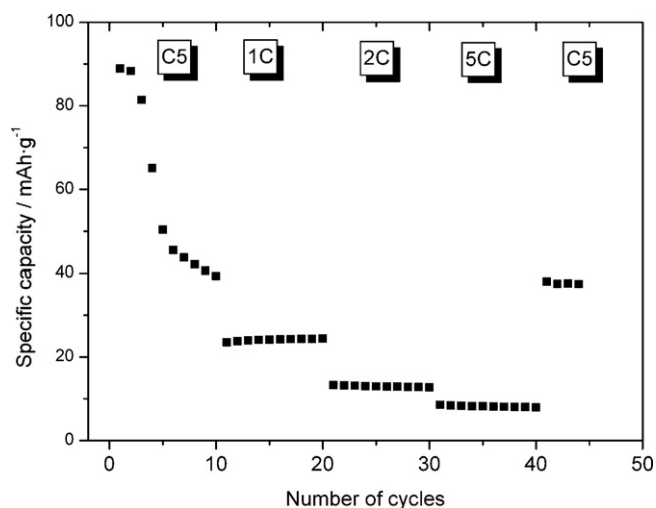


Fig. 5. Cycling behavior of a m- LiMn_2O_4 /5 M LiNO_3 /sm- LiV_3O_4 cell at different charge/discharge rates.

ical measurements beyond the scope of this communication. For this reason, our measurements of lithium cells were made on the micrometric sample.

The cathode/anode mole ratio used to assemble the cell was based on the theoretical capacity values for LiMn_2O_4 and LiV_3O_8 (148 and 272 mAh g^{-1} , respectively). Fig. 5 shows the variation of the discharge capacity of the cell as a function of the number of cycles at variable discharge rates from C/5 to 5C. The cell was made in a cathode/anode mole ratio of 3:1, equivalent to a capacity ratio of the positive (P) to the negative electrode (N) (P/N ratio) of 1.0, which is the recommended value for these electrochemical devices [19]. As can be seen, the delivered capacity at low rate (C/5), around 42 mAh g^{-1} , was somewhat lower than that obtained by Wang et al. [11] at the same rate and an unstated P/N ratio. Under these conditions, the capacity faded significantly on cycling to one-half the original value in the tenth cycle. We believe that such a poor performance is a result of the V-based compound being dissolved, clearly seen by disassembling the cell and observing the yellow color taken by the porous propylene film. Increasing the rate not only decreased the capacity (as expected), but also resulted in good capacity retention on cycling. Although we have no accurate model to interpret this peculiar behavior, we can put forward two plausible to explain it. Thus, cycling at low rates involves contact between the aqueous electrolyte absorbed on the propylene film and the particles of the V compound over a long enough for the dissolution process

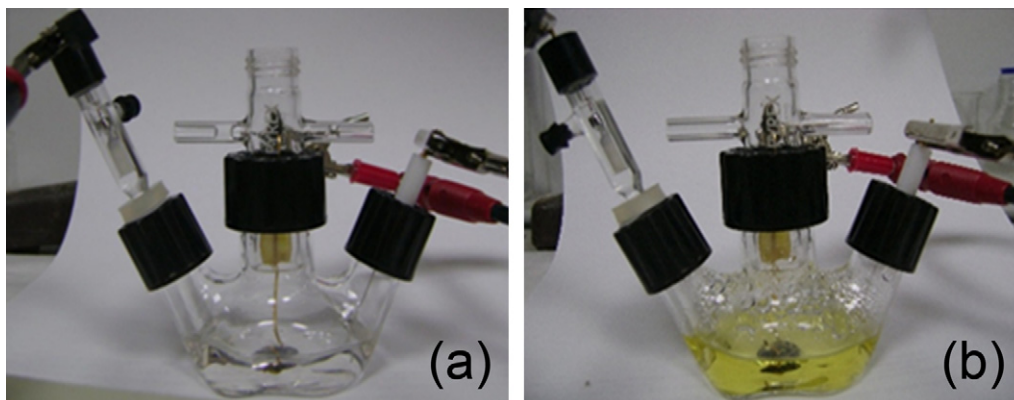


Fig. 4. Appearance of the electrolytic solution before (a) and during half-cell operation (b). The change from colorless to yellowish aspect is quite apparent.

to reach equilibrium. In fact, the slope of the capacity fading segment starts to decrease after the seventh cycle. On the other hand, increasing the charge/discharge rate reduces the contact period of electrolyte–active particles and hence the amount of material that is dissolved. Interestingly, lowering the charge/discharge rate from 5C to C/5 allowed the capacity to be recovered. The moderate capacity decline observed on further cycling somehow supports the former hypothesis. Even so, the good capacity retention observed at high rates cannot offset the very low capacity delivered by the cell under these conditions. Actions aimed at reducing or avoiding dissolution of the active material in the electrolyte, such as those proposed by Wang et al. [20], who coat particle surfaces with water-resistant agents, might provide an effective solution.

4. Conclusions

LiV_3O_8 is a well-known cathodic material for Li rechargeable batteries by virtue of its reversibly reaction with Li delivering a high specific capacity. This phenomenon is well documented in nonprotic solvents and has been ascribed to its layered structure. This was one of the main reasons to recommend and test it as an electrode material in aqueous rechargeable lithium batteries. These cells, however, have rather limited capacity retention. The origin of this shortcoming is quite simple: the compound is unstable under the typical operation conditions of the cell, where it dissolves in the electrolyte. Although the reason of this instability is unknown, a potential role of the intrinsic intercalation properties of the oxide cannot be ruled out. In fact, water molecules may be co-intercalated in the layered structure due to the high hydration tendency of Li^+ ions and resulting in structural expansion. The stress thus induced may exceed the flexibility of the structure and cause it to collapse, thereby facilitating its dissolution.

Acknowledgements

This work was performed with the financial support of the Ministerio de Ciencia e Innovación (Project MAT2008-03160) and Junta de Andalucía (Group FQM-175).

References

- [1] W. Li, J.R. Dahn, D.S. Wainwright, *Science* 264 (1994) 1115.
- [2] W. Li, W.R. McKinnon, J.R. Dahn, *J. Electrochem. Soc.* 141 (1994) 2310.
- [3] N. Li, C.J. Patrissi, G. Che, C.R. Martin, *J. Electrochem. Soc.* 147 (2000) 2044.
- [4] A. Eftekhari, *Electrochim. Acta* 47 (2001) 495.
- [5] M. Manickam, P. Singh, S. Thurgate, K. Prince, *J. Power Sources* 158 (2006) 646.
- [6] J.Y. Luo, Y.Y. Xia, *Adv. Funct. Mater.* 17 (2007) 3877.
- [7] R. Ruffo, C. Wessells, R.A. Huggins, Y. Cui, *Electrochem. Commun.* 11 (2009) 247.
- [8] J. Köhler, H. Makihara, H. Uegaito, H. Inoue, M. Toki, *Electrochim. Acta* 46 (2000) 59.
- [9] G.J. Wang, N.H. Zhao, L.C. Yang, Y.P. Wu, H.Q. Hu, R. Holze, *Electrochim. Acta* 52 (2007) 4911.
- [10] G.J. Wang, L.J. Fu, N.H. Zhao, L.C. Yang, Y.P. Wu, H.Q. Hu, *Angew. Chem. Int. Ed.* 46 (2007) 295.
- [11] G.J. Wang, H.P. Zhang, L.J. Fu, B. Wang, Y.P. Wu, *Electrochem. Commun.* 9 (2007) 1873.
- [12] G.J. Wang, L.J. Fu, B. Wang, N.H. Zhao, Y.P. Wu, R. Holze, *J. Appl. Electrochem.* 38 (2008) 579.
- [13] W. Li, J.R. Dahn, *J. Electrochem. Soc.* 142 (1995) 1742.
- [14] X.R. Ye, D.Z. Jia, J.Q. Yu, X.Q. Xin, Z. Xue, *Adv. Mater.* 11 (1999) 941.
- [15] J.C. Arrebola, A. Caballero, L. Hernán, J. Morales, E. Rodríguez Castellón, *Adv. Funct. Mater.* 16 (2006) 1904.
- [16] H. Wang, Y. Zeng, K. Huang, S. Liu, L. Chen, *Electrochim. Acta* 52 (2007) 5102.
- [17] A. Ott, P. Endres, V. Klein, B. Fuchs, A. Jäger, H.A. Mayer, S.K. Sack, H.W. Paas, K. Brandt, G. Filoti, V. Kunczer, M. Rosenberk, *J. Power Sources* 72 (1998) 1.
- [18] A.S. Aricò, P.G. Bruce, B. Scrosati, J.M. Tarascon, W.A. Schalkwijk, *Nat. Mater.* 4 (2005) 366.
- [19] K. Amine, J. Liu, S. Kang, I. Belharouak, Y. Hyung, D. Vissers, G. Henriksen, *J. Power Sources* 129 (2004) 14.
- [20] H. Wang, K. Huang, Y. Zeng, F. Zhao, L. Chen, *Electrochem. Solid State Lett.* 10 (2007) A199.